Kinetics of the $CCl_3 + CH_3$ Radical−Radical Reaction

Vadim D. Knyazev,* Irene R. Slagle, and Mikhail G. Bryukov[†]

Research Center for Chemical Kinetics, Department of Chemistry, The Catholic University of America, Washington, D.C. 20064

Received: October 29, 2002; In Final Form: February 12, 2003

The $CCl_3 + CH_3$ (1) cross-radical reaction was studied by laser photolysis/photoionization mass spectroscopy. Overall rate constants were obtained in direct real-time experiments in the temperature region 306−800 K and bath gas (helium) density region $(3-12) \times 10^{16}$ atoms cm^{-3}. The observed rate constant of reaction 1 is independent of temperature and equal to $(2.05 \pm 0.30) \times 10^{-11}$ cm^3 molecule^{-1} s^{-1}. Formation of $C_2H_2Cl_2$ and $C_2H_3Cl_2$ was detected; however, only the $C_2H_3Cl_2$ radical can be identified as a product of reaction 1 on the basis of the experimental information since the contribution of reaction 1 to the signal of $C_2H_2Cl_2$ could not be separated from that of the reaction of CCl_2 with CH_3 (CCl_2 being a minor product of photolysis of all precursors of CCl_3 used). The experimental values of the rate constant are in reasonable agreement with the prediction based on the "geometric mean rule". A separate experimental attempt to determine the rate constant of the high-temperature $CCl_3 + O_2$ (10) reaction resulted in the upper limit of $k_{10} \leq 3.0 \times 10^{-16}$ cm^3 molecule^{-1} s^{-1} at 800 K.

I. Introduction

Radical−radical cross-combination reactions constitute an integral part of the overall mechanisms of oxidation and pyrolysis of hydrocarbons.[1,2] Radical−radical reactions involving chlorinated methyl radicals are of particular importance in the mechanisms of combustion of chlorinated hydrocarbons. When compared to nonchlorinated radicals, chlorinated methyl radicals are characterized by increased kinetic stability in the combustion environment due to weaker C−O bonds in the peroxy adducts which are formed by the addition of the radical to the O_2 molecule (ref 3 and references therein). These weaker C−O bonds favor decomposition to O_2 and the chlorinated methyl radical as opposed to further transformations of the adduct. Since high-temperature reactions between chloromethyl radicals and O_2 are thus relatively slow, these radicals tend to accumulate in higher concentrations in flames, resulting in a greater importance of their reactions with other open-shell species, such as O, OH, hydrocarbon radicals, and H atoms.[4]

In processes of oxidation and pyrolysis of pure chlorinated methanes, the reactions between chlorinated methyl radicals are the only pathways to higher molecular mass products (C_2, C_3, etc.). In more complex systems involving oxidation of mixtures of methane/chlorinated methane (for example, $CH_2Cl_2/CH_4/O_2/Ar$ mixtures[5]), reactions between chlorinated methyl radicals and CH_3 become important and play the same role in molecular mass growth.[5−7] It was proposed by Granada et al.[8] that the rapid rates of these reactions can be used to purposefully promote formation of valuable products such as ethylene, acetylene, and vinyl chloride in the chlorine-catalyzed oxidative pyrolysis of methane.

Reliable knowledge of the rate constants of the chloromethyl + CH_3 reactions is needed to accurately predict high-molecular-mass product formation (including toxic byproducts) in the combustion and pyrolysis of chlorinated hydrocarbons. Despite the great importance and sensitivity of these reactions, almost no experimental information on them is available in the literature. The only experimental study of one reaction of this class is that of Garland and Bayes,[9,10] who used the laser photolysis/photoionization mass spectrometry technique to investigate several radical−radical reactions at room temperature and low pressures (4 Torr). Their attempt to determine the rate constant of the reaction

$$CCl_3 + CH_3 \rightarrow \text{products} \tag{1}$$

in argon bath gas resulted in an upper limit of $k_1 \leq 6 \times 10^{-12}$ cm^3 molecule^{-1} s^{-1}.

In general, reliable rate and branching data on radical−radical reactions are sparse as these reactions are difficult to study experimentally due to the high reactivity of the chemical species involved. Due to the lack of directly obtained experimental values, rate constants of cross-combination reactions are often estimated using the "geometric mean rule":[9,11,12]

$$k_{AB} = 2(k_{AA}k_{BB})^{1/2} \tag{I}$$

(Here, k_{AB} is the rate constant of the A + B reaction and k_{AA} and k_{BB} are the rate constants of the A + A and B + B self-reactions, respectively.) Validation of the geometric mean rule, however, is also problematic for the same reason, i.e., a deficit of directly obtained experimental rate constant values.

The upper limit of k_1 reported by Garland and Bayes seems to violate the geometric mean rule. Combination of the room-temperature high-pressure-limit rates of the reactions

$$CCl_3 + CCl_3 \rightarrow C_2Cl_6 \tag{2}$$

$$CH_3 + CH_3 \rightarrow C_2H_6 \tag{3}$$

(k_2^∞(298 K) = 3.3×10^{-12} [13] and k_3^∞(298 K) = 5.8×10^{-11}

---

* To whom correspondence should be addressed. E-mail: knyazev@cua.edu.

[†] Current address: Biodynamics Institute, Louisiana State University, 711 Choppin Hall, Baton Rouge, LA 70803.

10.1021/jp027335i CCC: $25.00

cm^3 molecule^{-1} s^{-1} [14]) results in the prediction of $k_1 \approx 2.8 \times 10^{-11}$ cm^3 molecule^{-1} s^{-1}, a much larger value than the upper limit of 6×10^{-12} cm^3 molecule^{-1} s^{-1} of refs 9 and 10.

In the current study, we report the results of an experimental investigation of reaction 1, that of the trichloromethyl (CCl_3) radical with CH_3. Reaction 1 was studied by means of laser photolysis/photoionization mass spectrometry at low bath gas densities ([He] = (3−12) × 10^{16} atoms cm^{-3}) in the 306−800 K temperature range. Overall rate constants were obtained in direct experiments by monitoring the real-time kinetics of both CCl_3 and the CH_3 radical. In a separate experimental investigation of the high-temperature reaction between CCl_3 and O_2, an upper limit of the rate constant was obtained at 800 K.

This paper is organized as follows. Section I is an introduction. Section II presents the experimental method and the results. A discussion is given in section III.

II. Experimental Section

In this section, the experimental apparatus used is described and the photolysis routes of the free radical precursors are characterized. The method of determination of rate constants and the associated kinetic mechanism is explained next, followed by a description of the experimental procedure used and that of the experimental results. Finally, a short study of the high-temperature reaction between CCl_3 and O_2, which resulted in an upper limit of the rate constant at 800 K, is presented.

II.1. Apparatus. Details of the experimental apparatus[15] and method[16−18] have been described previously. Only a brief description is presented here. Pulsed 193 nm unfocused collimated radiation from a Lambda Physik 201 MSC ArF excimer laser was directed along the axis of a 50 cm long 1.05 cm i.d. heatable tubular quartz reactor coated with boron oxide.[19] The laser was operated at 4 Hz; the energy flux of the laser radiation inside the reactor was in the range of 1−11 mJ pulse^{-1} cm^{-2} depending on the degree of laser beam attenuation.

Gas flowing through the tube at ~4 m s^{-1} (to replace the photolyzed gas with a fresh reactant gas mixture between the laser pulses) contained free radical precursors in low concentrations and the bath gas, helium. The gas was continuously sampled through a 0.04 cm diameter tapered hole in the wall of the reactor (gas-sampling orifice) and formed into a beam by a conical skimmer before it entered the vacuum chamber containing the photoionization mass spectrometer. As the gas beam traversed the ion source, a portion was photoionized using an atomic resonance lamp, mass selected in an EXTREL quadrupole mass filter, and detected by a Daly detector.[20] Temporal ion signal profiles were recorded from 10 to 30 ms before each laser pulse to 15−35 ms following the pulse by using a multichannel scaler. Typically, data from 500−10000 repetitions of the experiment were accumulated before the data were analyzed. The sources of ionizing radiation were chlorine (8.9−9.1 eV, CaF_2 window, used to detect CCl_3 and $C_2H_3Cl_2$), hydrogen (10.2 eV, MgF_2 window, used to detect CH_3, $C_2H_2Cl_2$, $(CH_3)_2CO$, and CCl_2), and argon (11.6−11.9 eV, LiF window, used in an attempt to detect CH_3CCl_3) resonance lamps.

II.2. Photolysis of Radical Precursors. Radicals were produced by the 193 nm photolysis of corresponding precursors. The photolysis of acetone at 193 nm, which was used in this study as the source of methyl radicals, was shown by Lightfoot et al.[21] to proceed predominantly (>95%) via channel 4a under conditions similar to those used in the current work. Photolysis channels 4b and 4c

$$CH_3C(O)CH_3 \xrightarrow{193\ \mathrm{nm}} 2CH_3 + CO \tag{4a}$$

$$\rightarrow H + CH_2C(O)CH_3 \tag{4b}$$

$$\rightarrow CH_4 + CH_2CO \tag{4c}$$

are known[21] to occur to a minor degree, <3% and <2%, respectively. The initial concentration of CH_3 radicals produced by the photolysis can thus be determined by measuring the photolytic depletion of $CH_3C(O)CH_3$, i.e., the fraction of acetone decomposed due to photolysis (see below).

Photolysis of three different precursors (perchloroacetone, carbon tetrachloride, and chloropicrin) was used to produce CCl_3 radicals:

$$(CCl_3)_2CO \xrightarrow{193\ \mathrm{nm}} 2CCl_3 + CO \tag{5a}$$

$$\rightarrow CCl_2 + \text{other products} \tag{5b}$$

$$\rightarrow \text{other products} \tag{5c}$$

$$CCl_4 \xrightarrow{193\ \mathrm{nm}} CCl_3 + Cl \tag{6a}$$

$$\rightarrow CCl_2 + 2Cl \tag{6b}$$

$$\rightarrow \text{other products} \tag{6c}$$

$$CCl_3NO_2 \xrightarrow{193\ \mathrm{nm}} CCl_3 + NO_2 \tag{7a}$$

$$\rightarrow CCl_2 + \text{other products} \tag{7b}$$

$$\rightarrow \text{other products} \tag{7c}$$

All three precursors of CCl_3 also produced CCl_2 as a side photolytic product.

Radical precursors were obtained from Aldrich (acetone (>99.9%), perchloroacetone (≥99%), carbon tetrachloride (>99.9%), and chloropicrin (≥98%)) and were purified by vacuum distillation prior to use. Helium (>99.999%, <1.5 ppm O_2, MG Industries) was used without further purification.

II.3. Method of Determination of Rate Constants. CH_3 and CCl_3 radicals were produced simultaneously by the 193 nm photolysis of a mixture of corresponding precursors highly diluted in the helium carrier gas (>99.7%). Rate constant measurements were performed using a technique analogous to that applied by Niiranen and Gutman to the studies of the $SiH_3 + CH_3$ and $Si(CH_3)_3 + CH_3$ kinetics,[22] and used by us recently to study the kinetics of the reactions of vinyl, allyl, propargyl, ethyl, n-C_3H_7, and n-C_4H_9 radicals with CH_3.[16−18] Experimental conditions (in particular, the two precursor concentrations) were selected to create a large excess of initial concentrations of methyl radicals over the total combined concentration of all the remaining radicals formed in the system. The initial concentration of methyl radicals was 14−117 times higher than that of CCl_3. The concentration of CCl_3 was always less than 1.8×10^{11} molecules cm^{-3}. Under these conditions, the self-recombination of methyl radicals was essentially unperturbed by the presence of other radicals. At the same time, the kinetics of CCl_3 decay was completely determined by the reaction with CH_3 and unaffected either by self-reaction or by reactions with other active species formed in the system, such as the side products of precursor photolysis.

Heterogeneous loss was the only additional sink of methyl and CCl_3 radicals that had to be taken into account. Thus, the kinetic mechanism of the important loss processes of CH_3 and CCl_3 in these experiments is as follows:

$$CCl_3 + CH_3 \rightarrow \text{products} \tag{1}$$

$$CH_3 + CH_3 \rightarrow C_2H_6 \tag{3}$$

$$CCl_3 \rightarrow \text{heterogeneous loss} \tag{8}$$

$$CH_3 \rightarrow \text{heterogeneous loss} \tag{9}$$

For this mechanism with the initial conditions described above, the system of first-order differential equations can be solved analytically:

$$\frac{[CH_3]_t}{[CH_3]_0} = \frac{k_9 \exp(-k_9 t)}{2k_3[CH_3]_0(1 - \exp(-k_9 t)) + k_9} \tag{II}$$

$$\frac{[CCl_3]_t}{[CCl_3]_0} = \exp(-k_8 t)\left[\frac{k_9}{2k_3[CH_3]_0(1 - \exp(-k_9 t)) + k_9}\right]^{k_1[CH_3]_0/2k_3[CH_3]_0} \tag{III}$$

Experimental signal profiles of CH_3 and CCl_3 radicals (see the Procedure subsection below) were fitted with eqs II and III, respectively, to obtain the values of the $k_3[CH_3]_0$ and the $k_1[CH_3]_0$ products. The k_1 rate constants were then obtained by dividing the experimental $k_1[CH_3]_0$ values by $[CH_3]_0$ determined by measuring the photolytic depletion of acetone (see below). An important feature of this method is that exact knowledge of the initial concentration of CCl_3 is not required for the determination of the rate constants. In this respect, the approach is similar to the pseudo-first-order method frequently applied to studies of kinetics of second-order reactions.

II.4. Procedure. In experiments with only one of the radical precursors present in the reactor under conditions where radical−radical reactions are negligible (low precursor concentration and/or low laser intensity), the radical kinetics (CH_3 or CCl_3) was that of purely exponential decay. The rate of the decay did not depend on the concentration of the precursor or the laser intensity but was affected by the wall conditions of the reactor (such as coating and history of exposure to reactive mixtures). This decay was attributed to heterogeneous loss processes. The rate constants of heterogeneous loss of methyl (k_9) and CCl_3 (k_8) radicals were determined in separate sets of measurements. The radical wall loss rates were in the range 0−15 s^{-1} and were minor compared to the rates of radical decay due to reactions 1 and 3.

In the experiments to measure the $CCl_3 + CH_3$ reaction rate constants, the initial (high) concentration of methyl radicals was determined by measuring the photolytic depletion of acetone (the fraction of acetone decomposed due to photolysis). The value of the decomposition ratio (the relative decrease in the precursor concentration upon photolysis) was obtained from the acetone ion signal profile (typical profiles are shown in Figure 1). In experiments where perchloroacetone was used as the photolytic precursor of CCl_3, initial concentrations of CCl_3 were evaluated by monitoring its photolytic depletion. Since products other than CCl_3 were also produced in the photolysis (reaction 5), only upper limit values to the concentration of CCl_3 could be obtained. In experiments with the CCl_4 and the CCl_3NO_2 precursors, the extent of photolytic depletion was too low to be accurately measured; therefore, $[CCl_3]_0$ values were estimated from the magnitudes of the CCl_3^+ ion signals.

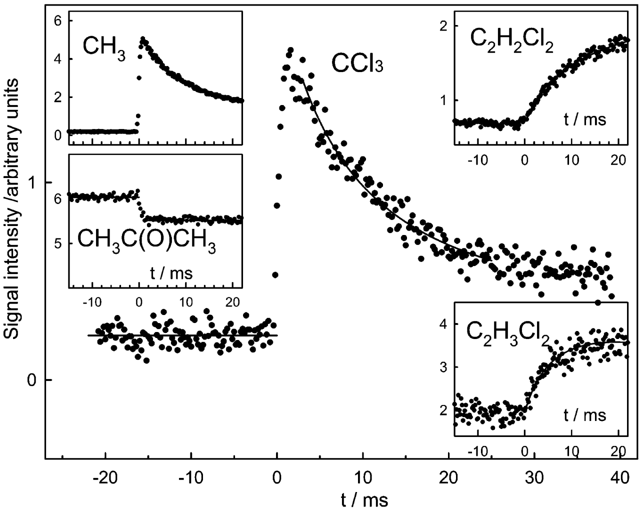

Figure 1. Example of a temporal ion signal profile of CCl_3 obtained in the experiments to measure k_1. Insets: profiles of CH_3, $CH_3C(O)CH_3$, $C_2H_2Cl_2$, and $C_2H_3Cl_2$ obtained in the same experiment. $T = 800$ K, $[He] = 1.20 \times 10^{17}$ atoms cm^{-3}, and $[CCl_3C(O)CCl_3] = 4.6 \times 10^{11}$, $[CH_3C(O)CH_3] = 3.35 \times 10^{13}$, $[CCl_3]_0 \leq 8.8 \times 10^{10}$, and $[CH_3]_0 = 5.82 \times 10^{12}$ molecules cm^{-3}.

The procedure of determination of the $CCl_3 + CH_3$ rate constants for each set of experimental conditions consisted of the following sequence of measurements.

(1) Kinetics of heterogeneous loss of CCl_3 (determination of k_8). Only the CCl_3 radical precursor is present in the reactor (along with the helium carrier gas, which is always present).

(2) Decomposition ratio of $(CCl_3)_2CO$ (determination of an upper limit of $[CCl_3]_0$). This step was not present in experiments where CCl_4 or CCl_3NO_2 was used as a precursor of CCl_3.

(3) Kinetics of heterogeneous loss of CH_3 (determination of k_9). Only acetone is in the reactor. The photolyzing laser beam is significantly attenuated to provide low CH_3 concentrations.

(4) Decomposition ratio of acetone (determination of $[CH_3]_0$). Both radical precursors are in the reactor from here to step 6. Low or no attenuation of the laser beam is used (high CH_3 concentrations) from here to step 6.

(5) Kinetics of methyl radical decay (determination of the $k_3[CH_3]_0$ product).

(6) Kinetics of CCl_3 radical decay in the presence of methyl radicals (determination of the $k_1[CH_3]_0$ product and k_1).

Measurements 4 and 5 were repeated in reverse order after the kinetics of CCl_3 radicals in the presence of methyl radicals was monitored to ensure the stability of initial concentrations of CH_3. The stability of the heterogeneous loss rate constants during the set of measurements was also checked experimentally.

Typical temporal profiles of $[CH_3C(O)CH_3]$ (photolytic precursor of CH_3 radicals), $[CH_3]$, and $[CCl_3]$ are shown in Figure 1. The lines through the experimental $[CH_3]$ and $[CCl_3]$ vs time profiles are obtained from fits of these dependences with expressions II and III, respectively. In each experiment (consisting of the set of measurements described above), the value of the $k_3[CH_3]_0$ product was obtained from the fit of the $[CH_3]$ vs time dependence (measured in step 5) using the value of k_9 (wall loss of CH_3) determined in step 3. Then the value of the $k_1[CH_3]_0$ product was obtained from the fit of the $[CCl_3]$ vs time dependence using the k_8, k_9, and $k_3[CH_3]_0$ values obtained in steps 1, 3, and 5, respectively. Finally, the value of

TABLE 1: Conditions and Results of Experiments To Determine the Rate Constants k_1 of the $CCl_3 + CH_3$ Reaction

T/K	[He][a]	[prec][b]	$[C_3H_6O]$[b]	$[CCl_3]_0$[b]	$[CH_3]_0$[b]	I[c]	k_8/s^{-1}	k_9/s^{-1}	k_3[d]	k_1[d]
306	12.0	4.5	117	0.7	10.6	10	5.8	10.0	2.68 ± 1.06	1.96 ± 1.06
306	12.0	4.5	288	0.8	27.6	11	7.8	10.0	2.76 ± 1.21	2.19 ± 1.04
400	3.0	13.5	631	0.6	25.5	5	0.5	7.5	1.95 ± 0.88	1.93 ± 0.69
400	3.0	13.5	318	0.5	10.4	4	0.5	7.5	2.02 ± 0.76	2.07 ± 0.77
400	3.0	25.4[e]	254	0.3[e]	21.1	9	2.1	1.6	2.38 ± 0.58	2.23 ± 0.89
500	3.0	44.3[f]	309	1.0[f]	36.0	6	4.5	7.8	1.79 ± 0.49	1.80 ± 0.67
600	3.0	24.2	695	1.8	43.9	5	0.2	9.1	1.18 ± 0.40	1.78 ± 0.44
600	3.0	24.2	725	0.4	10.4	1	0.2	9.1	0.98 ± 0.51	2.05 ± 1.05
600	12.0	4.6	111	0.5	17.0	11	0.4	3.0	2.00 ± 0.80	1.93 ± 0.58
800	3.0	9.7	737	1.1	79.6	6	0.2	8.7	0.43 ± 0.19	1.98 ± 0.54
800	3.0	9.7	213	0.8	16.2	4	0.1	8.3	0.53 ± 0.29	2.13 ± 0.57
800	3.0	4.5	351	1.0	66.3	11	-0.4	9.2	0.53 ± 0.19	2.49 ± 0.66
800	12.0	4.6	335	0.9	58.2	10	0.7	6.8	0.77 ± 0.18	2.06 ± 0.37
800	3.0	4.3	605	0.7	86.4	8	0.7	14.5	0.43 ± 0.23	2.00 ± 0.82

[a] Concentration of the bath gas (helium) in units of 10^{16} atoms cm^{-3}. [b] Concentrations of the CCl_3 radical photolytic precursor ($(CCl_3)_2CO$ unless specified otherwise), acetone, CCl_3, and CH_3 in units of 10^{11} molecules cm^{-3}. The concentration of CCl_3 is an upper limit (see the text). [c] Laser intensity in mJ $pulse^{-1}$ cm^{-2}. [d] In units of 10^{-11} cm^3 $molecule^{-1}$ s^{-1}. [e] CCl_4 was used as the photolytic precursor of CCl_3. The initial concentration of CCl_3 was estimated from the signal intensity. [f] CCl_3NO_2 was used as the photolytic precursor of CCl_3. The initial concentration of CCl_3 was estimated from the signal intensity.

k_1 was obtained by dividing the $k_1[CH_3]_0$ product by $[CH_3]_0$ determined in step 4.

The sources of error in the measured experimental parameters such as temperature, pressure, flow rate, signal count, etc. were subdivided into statistical and systematic and propagated to the final values of the rate constants using different mathematical procedures for propagating systematic and statistical uncertainties.[23] In particular, the effects of uncertainties in the heterogeneous radical decay rates and in the $k_3[CH_3]_0$ product on the derived k_1 values were evaluated for all experiments. The error limits of the experimentally obtained rate constant values reported in this work represent a sum of 2σ statistical uncertainty and estimated systematic uncertainty.

II.5. Experimental Results. The rate constants of reaction 1 (k_1) were determined at temperatures between 306 and 800 K and bath gas densities [He] = (3−12) × 10^{16} atoms cm^{-3}. The upper limit of the experimental temperature was determined by the appearance of a strong background signal at the mass of CCl_3 ($m/e = 117$), which can be attributed to either ion fragmentation or thermal decomposition of the precursor. Conditions and results of all experiments are listed in Table 1. It was verified experimentally that these rate constants did not depend on the photolyzing laser intensity, initial concentrations of CCl_3 and CH_3, or nature or concentration of the photolytic precursor of CCl_3. The rate constant of reaction 1 did not demonstrate any pressure dependence within the experimental uncertainties.

Although the measurement of k_3 (CH_3 recombination) was not the goal of the current work, the experiments provided rate constant values for the $CH_3 + CH_3$ reaction. Uncertainty in the k_3 values (Table 1) is rather high, up to 55% of the values, due to the fact that the experimental conditions were optimized for most accurate determination of k_1, not k_3. The results obtained are in good agreement with those previously measured.[16−18,24]

The observed rate constants demonstrate no dependence on temperature (Figure 2). If the values of k_1 obtained at different temperatures are averaged, one obtains a temperature-independent value:

$$k_1 = (2.05 \pm 0.30) \times 10^{-11}\ \mathrm{cm^3\ molecule^{-1}\ s^{-1}} \qquad (306{-}800\ \mathrm{K}) \quad \mathrm{(IV)}$$

The uncertainty of the k_1 value in eq IV (smaller than the error limits of individual determinations listed in Table 1) is composed by adding the 2σ statistical uncertainty resulting from averaging and the 10% average systematic component of the uncertainty of rate determination. This averaging, certainly, is meaningful only under the assumption of the true temperature independence of k_1, i.e., if it is assumed that k_1 is intrinsically independent of temperature, as opposed to a case of a weak temperature dependence masked by the experimental uncertainties and data scatter.

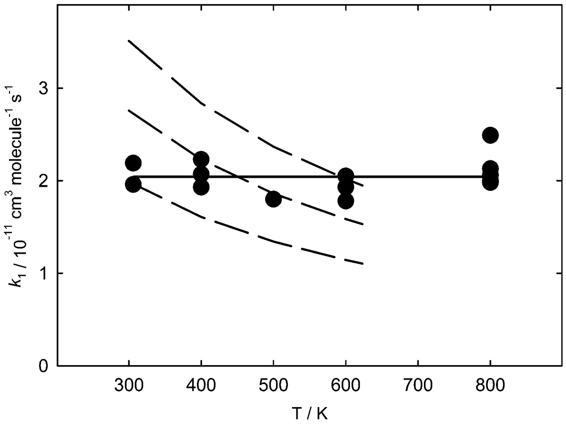

Figure 2. Temperature dependences of the rate constant of the $CCl_3 + CH_3$ reaction, k_1. Experimental values are shown by symbols. The horizontal solid line is the average temperature-independent value (eq IV). Three dashed lines show the central and the limiting values of k_1 calculated using the geometric mean rule, eq I.

Formation of $C_2H_3Cl_2$ and $C_2H_2Cl_2$ was detected in the experiments on reaction 1, at both the low and the high ends of the experimental temperature interval. The signal growth profiles of $C_2H_3Cl_2$ matched the decay of the CCl_3 radicals in reaction 1. Attempts to investigate the potential channel of formation of the CH_3CCl_3 adduct were unsuccessful because of the efficient fragmentation of the $CH_3CCl_3^+$ ion. The ionization potential of CH_3CCl_3 is ∼11.0 eV.[25] In separate experiments with measured flows of CH_3CCl_3, it was demonstrated that, when an argon resonance lamp (11.6−11.9 eV, LiF window) was used for photoionization, no signal at the parent mass ($m/e = 132$) could be detected. Instead, a fragmentation signal at $m/e = 97$ ($CH_3CCl_2^+$) was observed. This fragment ion signal could not be used to study formation of CH_3CCl_3 in reaction 1 because of the presence of the CH_3CCl_2 product at the same mass. Thus, no experimental information on the presence or absence of CH_3CCl_3 among the products of reaction 1 could be obtained. It can be ascertained that the $CH_3CCl_2^+$ signal ($m/e = 97$)

observed in the experiments on reaction 1 reflected formation of the CH_3CCl_2 radical (and did not originate from the fragmentation of CH_3CCl_3) because it was detected using a low-energy chlorine resonance lamp (8.9−9.1 eV, CaF_2 window).

As was mentioned above, all photolytic precursors of CCl_3 used in the current study also produced the CCl_2 biradical. Reaction of CCl_2 with CH_3 can be expected to produce the H + $C_2H_2Cl_2$ products via chemically activated decomposition of the excited CH_3CCl_2 adduct. Thus, it cannot be asserted with any degree of certainty whether the experimentally observed $C_2H_2Cl_2$ originates from both the $CCl_3 + CH_3$ and the $CCl_2 + CH_3$ reactions or only from the latter one. Stabilization of the CH_3CCl_2 adduct formed in the $CCl_2 + CH_3$ reaction is highly unlikely under the conditions of the current study (see the Discussion), and thus, the formation of the CH_3CCl_2 radical observed experimentally can only be attributed to reaction 1.

II.6. The $CCl_3 + O_2$ Reaction at 800 K. A separate short study of the high-temperature reaction between CCl_3 and O_2

$$CCl_3 + O_2 \rightarrow \text{products} \qquad (10)$$

was attempted at 800 K. The experimental conditions were similar to those used in the main part of this work, except for the absence of acetone and CH_3. No reaction could be detected. The upper limit value of $k_{10} \leq 3.0 \times 10^{-16}$ cm^3 molecule^{-1} s^{-1} was obtained by adding up to 3.4×10^{16} molecules cm^{-3} of O_2 (the concentration of He was reduced accordingly so that the total concentration of bath gas, $[He] + [O_2] = 1.2 \times 10^{17}$ molecules cm^{-3}, remained constant).

III. Discussion

III.1. Previous Work. This study presents the first direct determination of the rate constant of reaction 1 as a function of temperature. The only prior attempt at an experimental investigation of this reaction was undertaken by Garland and Bayes,[9,10] who used the laser photolysis/photoionization mass spectrometry (LP/PIMS) method similar to the one employed in the current investigation. However, many parameters of the equipment and experimental conditions were different, including the reactor geometry (a short, wider cylinder as opposed to a flow tube used in the current study), bath gas (Ar), and concentrations of radicals and precursors. Experiments were performed at room temperature only. These authors reported that they did not observe any changes to the rate of CCl_3 decay upon addition of large concentrations of CH_3, up to 7×10^{12} molecules cm^{-3}, and derived the upper limit of $k_1 \leq 6.0 \times 10^{-12}$ cm^3 molecule^{-1} s^{-1}.

The results of the current work ($k_1 = 2.05 \times 10^{-11}$ cm^3 molecule^{-1} s^{-1} at $T = 306-800$ K) contradict those reported by Garland and Bayes. This disagreement may seem surprising considering that reasonable agreement was observed previously between the room-temperature rate constants of refs 9 and 10 and our experimental results on the reactions of C_2H_5 and C_3H_5 radicals with CH_3.[17,18] One can suggest an explanation of the differences based on the role of molecular diffusion in the two experimental systems. In real-time experiments such as those described here and in refs 9 and 10, it is essential that a uniform concentration of reacting species is established on a time scale that is much shorter than the characteristic time scale of the reaction to be studied. For the LP/PIMS technique, this means that the diffusion of the radicals created by the laser photolysis must be significantly faster than their decay due to reaction. Garland[10] estimated the diffusion coefficient of the CCl_3 radical in argon bath gas for the conditions of the experiments of Garland and Bayes ($D(CCl_3/Ar) = 16.9$ cm^2 s^{-1} at 4 Torr) and the corresponding radial diffusion time ($t_D = 11.9$ ms). This diffusion time is longer than the typical time of the decay of CH_3 due to reaction 3 (∼5 ms) in the experiments of refs 9 and 10, which means that, by the time the uniform concentration of the CCl_3 radicals was established, the concentration of CH_3 radicals was already depleted. Thus, decay of CCl_3 due to reaction 1 could not be quantitatively studied. On the other hand, in the experiments performed in the current study, diffusion of CCl_3 was sufficiently fast to allow the determination of the rate constants. An estimation of the diffusion coefficient of CCl_3 in He using a method identical to that of Garland[10] yields the room-temperature value of $D(CCl_3/He) = 20.7$ cm^2 s^{-1} at 4 Torr and the characteristic radical diffusion time $t_D = 0.37$ ms. This diffusion time is much shorter that the typical decay times of CH_3 (>12 ms) and CCl_3. The differences in the values of the characteristic diffusion time between the current study and that of refs 9 and 10 is, primarily, due to the smaller diameter of the reactor used in the current work.

III.2. Reaction Products. Reaction 1 can proceed via three product channels, all involving formation of an excited $CH_3CCl_3^*$ intermediate:

$$CCl_3 + CH_3 \rightarrow CH_3CCl_3^* \rightarrow HCl + 1,1\text{-}C_2H_2Cl_2 \qquad (1a)$$

$$\rightarrow Cl + C_2H_3Cl_2 \qquad (1b)$$

$$\rightarrow CH_3CCl_3 \qquad (1c)$$

Enthalpies of these reaction channels can be evaluated as $\Delta H^\circ_{298}(1a) = -307.6 \pm 4.4$, $\Delta H^\circ_{298}(1b) = -47.8 \pm 10.5$, and $\Delta H^\circ_{298}(1c) = -361.9 \pm 4.5$ kJ mol^{-1} on the basis of the thermochemical information existing in the literature.[26−29] As was described in the previous section, formation of both $C_2H_2Cl_2$ and $C_2H_3Cl_2$ was observed, and formation of the CH_3CCl_3 adduct could not be experimentally confirmed or refuted because of the lack of sensitivity of the LP/PIMS apparatus to this species. All photolytic precursors of CCl_3 also produce the CCl_2 biradical, the reaction of which with CH_3 can proceed via two channels

$$CCl_2 + CH_3 \rightarrow CH_3CCl_2^* \rightarrow H + 1,1\text{-}C_2H_2Cl_2 \qquad (11a)$$

$$\rightarrow CH_3CCl_2 \qquad (11b)$$

with $\Delta H^\circ_{298}(11a) = -156.3 \pm 10.3$ and $\Delta H^\circ_{298}(11b) = -328.1 \pm 16.5$ kJ mol^{-1} (calculated using data from refs 26−28). It can be expected that the chemically activated decomposition channel 11a will be the only one occurring under the conditions of the current study, with stabilization (11b) playing no role because of the large difference between the entrance and the exit barriers.

Thus, the $C_2H_2Cl_2$ observed in the experiments is likely to originate, at least partially, from reaction 11a, and its formation in reaction 1a cannot be established on the basis of experimental information alone. On the other hand, observation of the CH_3CCl_2 radical proves the importance of channel 1b in reaction 1.

Thermal decomposition of CH_3CCl_3 is known to occur via both HCl elimination and Cl elimination,[30−34] although evaluations of the relative importance of these two channels differ. The Cl elimination pathway can be expected to have a relatively "loose" transition state compared to a "tighter" one for the HCl elimination. Thus, even if Cl elimination is a minor channel in the thermal decomposition of CH_3CCl_3, it can be expected to play a relatively more important role in the chemically activated dissociation of CH_3CCl_3, where competition between the two channels occurs at higher energies than in the case of a thermal reaction.

Experimental studies of CH_3CCl_3 pyrolysis report activation energies of 200−227 kJ mol^{-1} for thermal decomposition of CH_3CCl_3 via HCl elimination.[30−32,34] This barrier translates into a ∼130−165 kJ mol^{-1} gap between the entrance and the exit barriers in reaction channel 1a. A gap of ∼50 kJ mol^{-1} can be estimated for channel 1b. These large differences between the entrance and the exit barriers mean that any pressure dependence of the overall $CCl_3 + CH_3$ reaction is highly unlikely since all vibrationally excited adducts will either decompose to the products of channel 1a or 1b or stabilize by collisions with the bath gas. Absence of an observable pressure dependence of k_1 is in agreement with this conclusion.

III.3. Geometric Mean Rule. It is instructive to use the experimental temperature dependence of the rate constant of reaction 1 to test the validity of the geometric mean rule[9,11,12] (expression I) frequently used to estimate rate constants of cross-radical reactions (k_{AB}) of the type A + B from the values of k_{AA} and k_{BB}, the rate constants of the A + A and B + B self-reactions. As mentioned above, the experimental rate constant values of reaction 1 correspond to the high-pressure limit of the $CCl_3 + CH_3$ combination because decomposition of the vibrationally excited CCl_3CH_3 adduct back to reactants will be suppressed by competition with the much faster channels 1a and 1b (HCl and Cl elimination, respectively). The rate constants of the methyl radical self-reaction (reaction 3) are well-known. Two recent "global fits" [14,35] of falloff data provide parametrization for the rate constants that differ very little (less than 5%) in the high-pressure limit. A large part of the experimental data used in these parametrizations come from the experimental study of Slagle et al.,[24] who used the experimental technique and the apparatus employed in the current work. These authors reported a ±20% uncertainty in their experimental rate constant values. Thus, in the calculations according to the geometric mean rule, we used the parametrization of Hessler and Ogren[14] (k_3^{∞}(298 K) = 5.81×10^{-11} cm^3 $molecule^{-1}$ s^{-1}) with 20% uncertainty. The rate of the self-reaction of CCl_3 radicals

$$CCl_3 + CCl_3 \rightarrow C_2Cl_6 \tag{12}$$

has been determined by Danis et al.[13] in their flash photolysis/kinetic UV spectroscopy study in the 253−623 K temperature range. These authors reported a $k_{12}(T) = (3.3 \times 10^{-12})(T/298\ K)^{-1.0}$ cm^3 $molecule^{-1}$ s^{-1} temperature dependence. The statistical uncertainties of k_{12} reported by Danis et al. are, on average, ∼10%; the systematic uncertainty due to that of the UV cross-section of CCl_3 is estimated by the authors as ∼25%. Therefore, we use the expression of ref 13 for k_{12} with a 35% overall uncertainty.

The resultant k_1 temperature dependence calculated via eq I (the geometric mean rule) using the literature values of k_3 and k_{12} is shown in Figure 2. The upper and lower limiting values were calculated using the upper and lower limits of k_3 and k_{12}. The calculated $k_1(T)$ dependence is in reasonable agreement with the experimental values obtained in this work over the range of temperatures where information on both k_3 and k_{12} is available. However, the calculated and the experimental $k_1(T)$ dependences exhibit different temperature trends: the calculated values decrease with temperature, while the experimental results are temperature-independent. Nevertheless, the uncertainty limits of the calculations are sufficiently large to encompass all the experimental data points. If the trend of the calculated $k_1(T)$ dependence is continued to the highest temperature of the current experimental work, 800 K, then the 800 K experimental values of k_1 will fall out of the uncertainty envelope of the calculations. However, experimental data on reaction 12 are not available at 800 K. Also, the uncertainty of the high-pressure-limit values of k_3 can be expected to be larger at 800 K than at lower temperatures because they are obtained via extrapolation over larger pressure ranges,[14] and the 20% uncertainty assumed here for k_3^{∞} may be an underestimation. Thus, no definite conclusions can be reached regarding the adequacy of the geometric mean rule calculations at 800 K.

III.4. High-Temperature $CCl_3 + O_2$ Reaction. At low temperatures, the main channel of the reactions of chlorinated methyl radicals with O_2 is reversible addition to form an RO_2 peroxy radical ($R + O_2 \rightleftarrows RO_2$). The reaction of CCl_3 with O_2 has been extensively studied experimentally in both the low-temperature (addition) and the intermediate-temperature (relaxation to equilibrium) regions.[36−40] However, no rate constant measurements have been reported at higher temperatures, where equilibrium in the addition step is shifted to the left and the overall reaction (if any) is dominated by the rearrangement of the excited peroxy adduct. Ho et al.[4,41] studied the high-temperature reaction of chloromethyl radical with O_2

$$CH_2Cl + O_2 \rightleftarrows CH_2ClOO \rightarrow CH_2O + ClO \tag{13}$$

using the computational QRRK method; their estimated temperature dependence of k_{13} results in the value of $k_{13} \approx 6 \times 10^{-14}$ cm^3 $molecule^{-1}$ s^{-1} at 800 K. The mechanisms of the reactions of all chlorinated methyl radicals with O_2 at high temperatures can be expected to be similar. On the basis of analogy with reaction 13, the high-temperature reaction of CCl_3 with O_2 (reaction 10) can be expected to proceed via formation of the CCl_3OO adduct with its subsequent rearrangement and decomposition into phosgene (CCl_2O) and ClO. The results of the current study demonstrate that, if such a reaction takes place, its rate constant at 800 K is at least 2 orders of magnitude lower than the estimate of refs 4 and 41 for reaction 14. It should be noted that the CCl_3 radical is more stable than CH_2Cl by approximately 32 kJ mol^{-1} (relative to their respective ROO adducts),[3] which, if used in the van't Hoff factor, translates into a factor of 100 at 800 K. This stability of CCl_3 may account for the difference between the estimated high-temperature value of k_{13} and the experimental upper limit of the rate constant of reaction 10 at 800 K.

Acknowledgment. This research was supported by the National Science Foundation, Combustion and Thermal Plasmas Program, under Grant No. CTS-0105239.

References and Notes

(1) Tsang, W.; Hampson, R. F. *J. Phys. Chem. Ref. Data* **1986**, *15*, 1087.

(2) Warnatz, J. In *Combustion Chemistry*; Gardiner, W. C., Jr., Ed.; Springer-Verlag: New York, 1984.

(3) Knyazev, V. D.; Slagle, I. R. *J. Phys. Chem. A* **1998**, *102*, 1770.

(4) Ho, W. P.; Yu, Q.-R.; Bozzelli, J. W. *Combust. Sci. Technol.* **1992**, *85*, 23.

(5) Qun, M.; Senkan, S. M. *Combust. Sci. Technol.* **1994**, *101*, 103.

(6) Tavakoli, J.; Chiang, H. M.; Bozzelli, J. W. *Combust. Sci. Technol.* **1994**, *101*, 135.

(7) Karra, S. B.; Senkan, S. M. *Ind. Eng. Chem. Res.* **1988**, *27*, 447.

(8) Granada, A.; Karra, S. B.; Senkan, S. M. *Ind. Eng. Chem. Res.* **1987**, *26*, 6, 1901.

(9) Garland, L. J.; Bayes, K. D. *J. Phys. Chem.* **1990**, *94*, 4941.

(10) Garland, L. J. Determination of the Rate Constants for Radical−Radical Cross Reactions. Ph.D. Dissertation, University of California at Los Angeles: Los Angeles, CA, 1989.

(11) Kerr, J. A.; Trotman-Dickenson, A. F. *Prog. React. Kinet.* **1961**, *1*, 105.

(12) Blake, A. R.; Henderson, J. F.; Kutschke, K. O. *Can. J. Chem.* **1961**, *39*, 1920.

(13) Danis, F.; Caralp, F.; Veyret, B.; Loirat, H.; Lesclaux, R. *Int. J. Chem. Kinet.* **1989**, *21*, 715.

(14) Hessler, J. P.; Ogren, P. J. *J. Phys. Chem.* **1996**, *100*, 984.

(15) Slagle, I. R.; Gutman, D. *J. Am. Chem. Soc.* **1985**, *107*, 5342.

(16) Stoliarov, S. I.; Knyazev, V. D.; Slagle, I. R. *J. Phys. Chem. A* **2000**, *104*, 9687.

(17) Knyazev, V. D.; Slagle, I. R. *J. Phys. Chem. A* **2001**, *105*, 3196.

(18) Knyazev, V. D.; Slagle, I. R. *J. Phys. Chem. A* **2001**, *105*, 6490.

(19) Krasnoperov, L. N.; Niiranen, J. T.; Gutman, D.; Melius, C. F.; Allendorf, M. D. *J. Phys. Chem.* **1995**, *99*, 14347.

(20) Daly, N. R. *Rev. Sci. Insrum.* **1960**, *31*, 264.

(21) Lightfoot, P. D.; Kirwan, S. P.; Pilling, M. J. *J. Phys. Chem.* **1988**, *92*, 4938.

(22) Niiranen, J. T.; Gutman, D. *J. Phys. Chem.* **1993**, *97*, 9392.

(23) Bevington, P. R. *Data Reduction and Error Analysis for the Physical Sciences*; McGraw-Hill: New York, 1969.

(24) Slagle, I. R.; Gutman, D.; Davies, J. W.; Pilling, M. J. *J. Phys. Chem.* **1988**, *92*, 2455.

(25) Lias, S. G.; Bartmess, J. E.; Liebman, J. F.; Holmes, J. L.; Levin, R. D.; Mallard, W. G. *J. Phys. Chem. Ref. Data* **1988**, Suppl. 1, 1.

(26) Kerr, J. A. In *CRC Handbook of Chemistry and Physics*; Lide, D. R., Ed.; CRC Press: Boca Raton, FL, 1994−1995.

(27) Chase, M. W., Jr. *J. Phys. Chem. Ref. Data* **1998**, Monogr. 9, 1.

(28) Mansson, M.; Ringner, B.; Sunner, S. *J. Chem. Thermodyn.* **1971**, *3*, 547.

(29) Hu, A. T.; Sinke, G. C.; Mintz, M. J. *J. Chem. Thermodyn.* **1972**, *4*, 239.

(30) Barton, D. H. R.; Onyon, P. F. *J. Am. Chem. Soc.* **1950**, *72*, 988.

(31) Benson, S. W.; Spokes, G. N. *Symp. Int. Combust. Proc.* **1967**, *11*, 95.

(32) Dai, H.-L.; Specht, E.; Berman, M. R. *J. Chem. Phys.* **1982**, *77*, 4494.

(33) Holbrook, K. A.; Oldershaw, G. A.; Matthews, M. *Int. J. Chem. Kinet.* **1985**, *17*, 1275.

(34) Huybrechts, G.; Hubin, Y.; Van Mele, B. *Int. J. Chem. Kinet.* **1989**, *21*, 575.

(35) Robertson, S. H.; Pilling, M. J.; Baulch, D. L.; Green, N. J. B. *J. Phys. Chem.* **1995**, *99*, 13452.

(36) Cooper, R.; Cumming, J. B.; Gordon, S.; Mulac, W. A. *Radiat. Phys. Chem.* **1980**, *16*, 169.

(37) Ryan, K. R.; Plumb, I. C. *Int. J. Chem. Kinet.* **1984**, *16*, 591.

(38) Nottingham, W. C.; Rudolph, R. N.; Andrews, K. P.; Moore, J. H.; Tossell, J. A. *Int. J. Chem. Kinet.* **1994**, *26*, 749.

(39) Fenter, F. F.; Lightfoot, P. D.; Niiranen, J. T.; Gutman, D. *J. Phys. Chem.* **1993**, *97*, 5313.

(40) Russell, J. J.; Seetula, J. A.; Gutman, D.; Danis, F.; Caralp, F.; Lightfoot, P. D.; Lesclaux, R.; Melius, C. F.; Senkan, S. M. *J. Phys. Chem.* **1990**, *94*, 3277.

(41) Ho, W. P.; Barat, R. B.; Bozzelli, J. W. *Combust. Flame* **1992**, *88*, 265.